Journal of Solid Mechanics Vol. 14, No. 4 (2022) pp. 468-476
DOI: 10.22034/jsm.2021.1929196.1693

Research Paper

The Modelling of the Mechanics of Deformation in Plane Strain Upsetting of Round Cross-Section Billets Between the Flat and V-Shaped Dies

M. Maleki, H. Haghighat *

Mechanical Engineering Department, Razi University, Kermanshah, Iran

Received 23 July 2022; accepted 26 September 2022

ABSTRACT

Plane strain upsetting of round cross-section billets between the flat and V-shaped dies has been studied in this paper. A deformation model has been proposed and the geometry of the deformed billet cross-section is determined for a given displacement of the top flat die. To analyze the process, the slab method of analysis has been applied and for a given process conditions, the required forming load has been estimated. The process under consideration has been performed also with the finite-element method to predict the forming load and the material flow. The calculated forming load and the deformed billet cross-section geometry compare well with the FE simulations data. The effects of friction factor and the angle of the V-shaped bottom die on the forming load have been investigated. The theoretical results have been indicated that as the bottom die angle decreases the forming load decreases and the forming load is not influenced by friction in case of small bottom die angles.

Keywords : Plane strain upsetting; Deformation model; Slab method; Forming load.

1 INTRODUCTION

PLANE strain upsetting is a plastic deformation process in which an initial long billet is compressed by an external load applied by an upper die and is forced to plastically deform in the space between the moving upper and the stationary lower dies. This technological operation, is used as a preform operation in closed die forging of long billets. Different combinations of dies can be used for this metal forming process. In this study, flat and V-shaped dies are used as upper and lower dies, respectively. V-shaped die usage leads to the closing of defects during forging [1]. Exact solutions for the deformation of the material during the metal forming processes are not yet well established, except for a few cases. As well as in other processes, many advantages are provided by a sufficient knowledge of the mechanics of the deforming material in plane strain upsetting process. Conventionally, the geometry of the deformed shape and required upsetting load for each press stroke are unknowns. Estimation of the upsetting load is required for selecting of the press with enough capacity. It is desirable, therefore, to develop some

* Corresponding author. Tel.: +98 83 34343002; Fax: +98 83 34343194.
E-mail address: hhaghighat@razi.ac.ir (H. Haghighat)

simple but efficient methods to facilitate the prediction of the deformed shape of the billet and the load in plane strain upsetting process. A number of studies in the past using analytical models and the finite element method have been conducted on plane strain upsetting process. Based on practical experience of Nasmyth [2], he found that a V-shaped lower die was superior to a flat lower die regarding closure of centerline porosities and to ensure soundness of the final product. A theoretical analysis of the open die forging process using V-shaped and flat dies presented by Johnson [3], who applied slipline analysis for die compression of circular cylindrical billets. Upper bound analysis of compression of cylindrical billets with square cross section containing porosities was presented in Keife and Stahlberg [4] and corresponding model wax experiments in Stahlberg et al. [5]. Vilotic and Shabaik [6] presented a stress analysis for upsetting of block ingot by half-cylindrical dies. The slab method was used to examine the variation of stress distribution in deformation zone and the estimation of the variation of the press load as a function of die stroke. Dudra & Im [7] carried out plane strain numerical simulation of open die forging of model ingots with a centerline hole to mimic a porosity using a pair of plane and a pair of V-shaped 135o dies. They confirmed the aforementioned work of Nasmyth and Johnson that V-shaped dies were superior to plane dies regarding closure of centerline porosities. Dudra et al. [8] performed axisymmetric upsetting and plane-strain analyses with the finite-element method to predict the press load and material flow when forging with different die and billet geometries. Lin [9] used the rectangular slab method in conjunction with assumption of plane strain to determine the stress distribution within the deformation zone by concave curve dies. Choi et al. [10] performed a three-dimensional rigid-plastic finite element method (FEM) analysis to optimize an open die forging process in the production of circular shapes. Alexandrov and Yusof [11] proposed a simplified approach based on the upper bound theorem has for quick analysis and design of continued deformation of plane strain compression of a rectangular cross-section billet. A numerical study was presented by Christiansen et al. [12]. A real size ingot with a porous center region was compressed in a number of forging steps using a flat and a 90 V-shaped lower die. It was found that the flat lower die resulted in hydrostatic tension at the center of the ingot while the V-shaped die was able to suppress the hydrostatic tension hereby preventing porosity increase at the center of the ingot. Banaszek et al. [13] presented the results of numerical modelling of the forging process of magnesium alloy ingots on a hydraulic press with the use of flat and shaped dies. The objective of the study was to determine strain distributions in AZ91 magnesium alloy bars elongated with the open die forging method. Summarizing, it can be noticed that the mechanics of deformation in upsetting process of the horizontal long cylindrical billets between the flat and V-shaped dies, has not been addressed adequately.

The main objective of this paper is to use of the analytical method based on slab method of analysis for predicting of the deformed shape of the billet cross-section and the forming load for each press stroke. The process under consideration has been performed also with the finite-element method, by using DEFORM 2D software and the results are used to evaluate the accuracy of present model.

2 ANALYTICAL MODELLING

2.1 Geometric representation of the process

The plane strain upsetting process of horizontal round billets at the start of the operation is schematically illustrated in Fig. 1. In this process, the billet compresses between a moving flat top die and a V-shaped stationary bottom die. In this figure, angle θ is the angle of the bottom die surface with the horizontal direction and the initial radius of the billet is R_0.

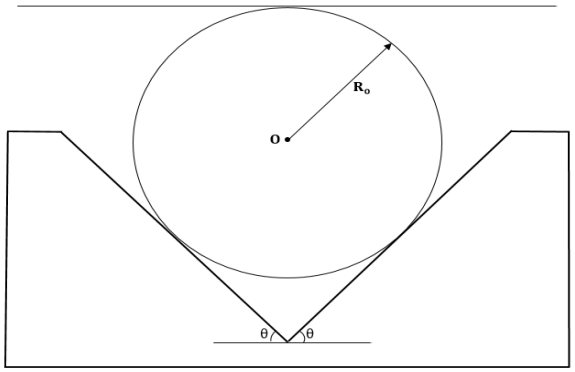

Fig.1
The configuration of the dies and the billet at the start of the operation.

Fig. 2 shows the process at a given stage of the operation. In this figure, δ_u is the vertical displacement of the upper flat die, δ_o is the vertical displacement of the center *O*, *b* is the half contact length between the upper die and the billet and *R* and R' are the radii of free surfaces BC and FG, respectively. The deformation proceeds with increasing of contact lengths between the billet and the dies surfaces as the upper flat die moves down. Due to the symmetry of the process as shown in Fig. 2, it is sufficient to find the solution only at the half-right of the billet cross-section.

The volume constancy principle is used to determine the contact lengths between the dies and the billet during the process. Based on the said principle, the cross-section areas of the billet before
and after a given displacement of the top die, must be equal, so:

$$\frac{1}{2}\pi R_0^{\,2} = \frac{1}{2}R^2\alpha + \frac{1}{2}b\left(R_0 - \delta_u + \delta_o\right) + \frac{1}{2}R'^2\alpha + \frac{1}{2}b\left(R_0 - \delta_u + \delta_o\right)\cos\theta \tag{1}$$

It is assumed that the new position of center *O*, point O', is located on the bisector of angle *T* as:

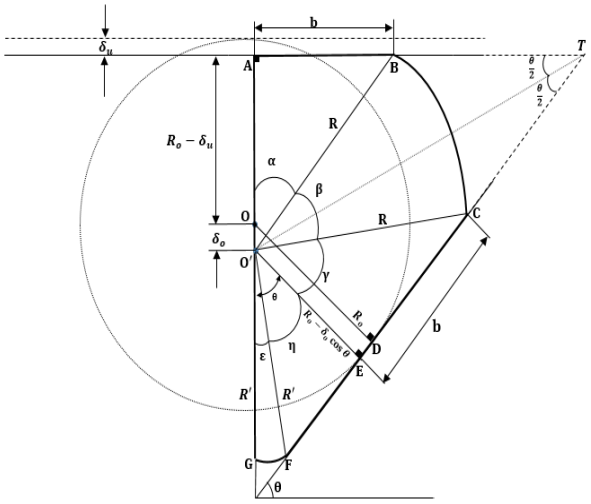

Fig.2
The configuration of the dies and the billet at a given upper die displacement.

Shown in Fig. 2, and we have

$$\delta_o = \frac{\delta_u}{1+\cos\theta} \tag{2}$$

The radius of the arc BC, *R* after downward displacement of top die as δ_u, can be related to the initial radius of the billet as:

$$R^2 = b^2 + \left(R_0 - \delta_u + \delta_o\right)^2 \tag{3}$$

The angle α can be given by

$$\alpha = \tan^{-1}\frac{R_0 - \delta_u + \delta_o}{b} \tag{4}$$

2.2 Slab analysis

The slab method of analysis is among the most popular techniques adopted in analyzing the plastic deformation of metallic materials. In the development of the slab solution, it is assumed that the dies are rigid and the material being

upset is rigid perfectly plastic. The plastic deformation occurs under plane strain condition. The friction factor is the same for all interfaces between the die and the material.

2.2.1 Stress state in the deformation zones

To analyze the process, the material in the deformation region is divided into three deformation regions (shown in Fig. 3 (a)) based on the material flow observed from the FE simulation. The cylindrical and Cartesian coordinate systems are used to carry out the analysis. The origins of cylindrical and Cartesian coordinate systems have been taken at point *O* as shown in Fig. 3(a).

The various stresses on the small elements taken from deformations zones I and II are shown in Figs. 3(b) and 3(c). The analysis proceeds as follows:

Region I. For this region, a cylindrical state (r,θ,z) of stress at a small element as shown in Fig. 3(b) is assumed. The stresses distributed within the element are uniform. It has been assumed that the σ_r is independent of θ. The radial stress σ_r and the circumferential stress σ_θ are regarded as principal stresses. The shear stress at the top and bottom surfaces is $\tau_{r\theta}$. Assuming a depth of "1" or unit length and by resolving the various forces due to the stresses acting on the slab element along the *x*-direction and for the equilibrium gives

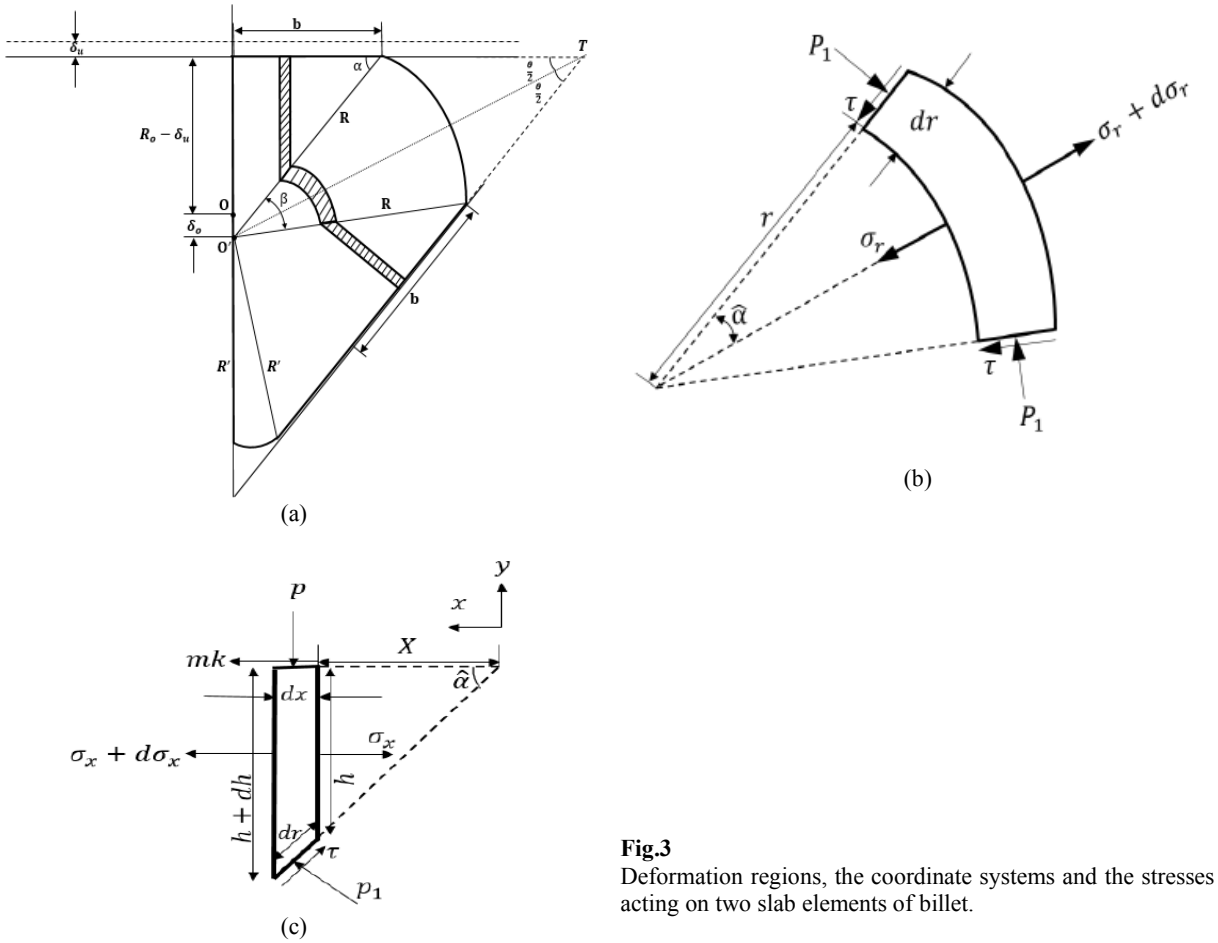

Fig.3
Deformation regions, the coordinate systems and the stresses acting on two slab elements of billet.

$$2\int_0^{\alpha}(\sigma_r + d\sigma_r)(r+dr)\cos\theta\, d\theta - 2\int_0^{\alpha}\sigma_r\, r\cos\theta\, d\theta + 2\sigma_\theta\, dr\sin\alpha - 2\tau_{r\theta}\, dr\cos\alpha = 0 \tag{5}$$

Neglecting the higher-order small quantities and simplifying, we have

$$r\frac{d\sigma_r}{dr}+\sigma_r+\sigma_\theta-\frac{\tau_{r\theta}}{\tan\alpha}=0 \tag{6}$$

The surface BC is traction free and the radial stress vanishes at $r=R$. The von Misses yield criterion has been adopted by most researchers. With the assumption of plane strain deformation in the process, these stresses can be related:

$$\sigma_r+\sigma_\theta=2k \ , \ d\sigma_r=-d\sigma_\theta \tag{7}$$

where k is the plane-strain shear flow stress of the billet material. By substituting Eq. (7) into Eq. (6), the following differential equation is obtained

$$r\frac{d\sigma_\theta}{dr}+\frac{\tau_{r\theta}}{\tan\alpha}-2k=0 \tag{8}$$

Region II. The state of stress on a slab of infinitesimal thickness in this region based on the Cartesian coordinate system is shown in Fig. 3(c). The friction between the die and the billet is assumed to be constant shear friction, $\tau=mk$, where the constant friction factor, m , can take on values from 0 to 1. The shear stress at the bottom surface is $\tau_{r\theta}$. The force equilibrium in the *y* direction gives:

$$p\,dx=\tau_{r\theta}\,dr\sin\alpha+\sigma_\theta\,dr\cos\alpha \tag{9}$$

Replacing dx by $dr\cos\alpha$, in the above equation, we have

$$p=\tau_{r\theta}\tan\alpha+\sigma_\theta \tag{10}$$

By differentiating of the Eq. (10) with respect to the variable *r*, we have

$$\frac{dp}{dr}=\frac{d\tau_{r\theta}}{dr}\tan\alpha+\frac{d\sigma_\theta}{dr} \tag{11}$$

By assuming a von Misses yield criterion, a relationship between the pressure p and σ_x (positive when under tension) can be established as:

$$\sigma_x+p=2k\,,d\sigma_x=-dp \tag{12}$$

Next, considering the force equilibrium along the *x*-axis, the following relationship is obtained

$$\left(\sigma_x+d\sigma_x\right)\left(h+dh\right)-\sigma_x\,h+mk\,dx+\sigma_\theta\,dr\sin\alpha-\tau_{r\theta}\,dr\cos\alpha=0 \tag{13}$$

By neglecting the higher-order small quantities and simplifying, we have

$$\sigma_x dh+hd\sigma_x+mk\,dx+\sigma_\theta\,dr\sin\alpha-\tau_{r\theta}\,dr\cos\alpha=0 \tag{14}$$

From Fig. 3(c) we have

$$dh=dr\sin\alpha \ , \ h=(b-r\cos\alpha)\tan\alpha \tag{15}$$

By placing p and dp from Eqs. (12) and (15) into Eq. (14), the differential Eq. (13) can be written as the following form

$$-\left(b-r\cos\alpha\right)\tan\alpha\frac{dp}{dr}+\left(2k-p\right)\sin\alpha+mk\cos\alpha+\sigma_\theta\sin\alpha-\tau_{r\theta}\cos\alpha=0 \tag{16}$$

By substituting p from Eq. (8) and $\frac{dp}{dr}$ from Eq. (11) into Eq. (16), we have

$$-\left(b-r\cos\alpha\right)\tan\alpha\left(\frac{d\tau_{r\theta}}{dr}\tan\alpha+\frac{d\sigma_\theta}{dr}\right)+\left[2k-\left(\tau_{r\theta}\tan\alpha+\sigma_\theta\right)\right]\sin\alpha+mk\cos\alpha+\sigma_\theta\sin\alpha-\tau_{r\theta}\cos\alpha=0 \tag{17}$$

By eliminating of $\tau_{r\theta}$ between Eqs. (8) and (17), the variation of σ_θ with the radial distance r is obtained as the second-order differential equation in the following form

$$f\left(r\right)\frac{d^2\sigma_\theta}{dr^2}+g\left(r\right)\frac{d\sigma_\theta}{dr}-k\left(2\sin^3\alpha-m\cos^3\alpha\right)=0 \tag{18}$$

In which

$$\begin{aligned} f\left(r\right)&=\frac{R_0-\delta_u+\delta_o}{b}\left(b-r\cos\alpha\right)r\sin^2\alpha \\ g\left(r\right)&=r\sin\alpha-\frac{R_0-\delta_u+\delta_o}{b}\left(b-r\cos\alpha\right)\cos2\alpha \end{aligned} \tag{19}$$

2.2.2 Forming load

From the above known distribution of pressure on the contact interface between the die and the billet material, it is possible to calculate the forming load per unit width F at any stage of deformation as:

$$F=2\sum_1^n P_i\Delta x_i \tag{20}$$

For a given process condition, the forming load is a function of δ_o, where it varies between 0 to δ_u. In the developed slab analysis, the minimum value of external load with respect to δ_o is the required load for upsetting process. The fourth-order Runge-Kutta methods are used in computer solutions to differential equations derived in the previous section. Based on these numerical methods, a MATLAB program was developed for the determination of the contact length, distribution of the pressure on contact length and corresponding required forming load for each stroke. Initial billet radius, bottom die angle, friction factor, stroke and the billet material properties are inputs of the established computer program.

3 FINITE ELEMENT SIMULATION

In order to validate the present analytical results, the numerical simulation of the process is conducted. In this study, the finite element analysis software DEFORM 2D ver11.0 is used to simulate the upsetting process of long cylindrical billets. The top and bottom dies are modeled as discrete rigid bodies and the billet material is assumed as perfect plastic material. The billet model was meshed with C3D8R elements and consists of a 4-node bilinear. These characteristics are appropriate for this element to be used in this type of analysis, where large deformations and contact nonlinearities are assumed. The dies are assumed as rigid bodies and they are not meshed. However,

sufficiently fine meshing is essential in material, which undergoes plastic deformation. The bottom die is fixed and the upper flat die, is moved in the vertical direction toward the bottom V-shaped die with constant velocity.

4 RESULTS AND DISCUSSION

The billet investigated is considered to be 10 *mm* in radius. The friction factor 0.1 and a rigid-perfectly plastic material, $2k = 100\,MPa$ are specified in this study. The billet is placed between a flat upper die and a V-shaped bottom die with angle $\theta = 45^{\circ}$. The upsetting speed $v_0 = 1$ *mm/s* are adopted during the analytical solution and the FEM simulation. Fig. 4 shows the schematic illustration of the billet cross-section model after upsetting using bottom die angle 45 for $\delta = 1, 2$ and 3 *mm*.

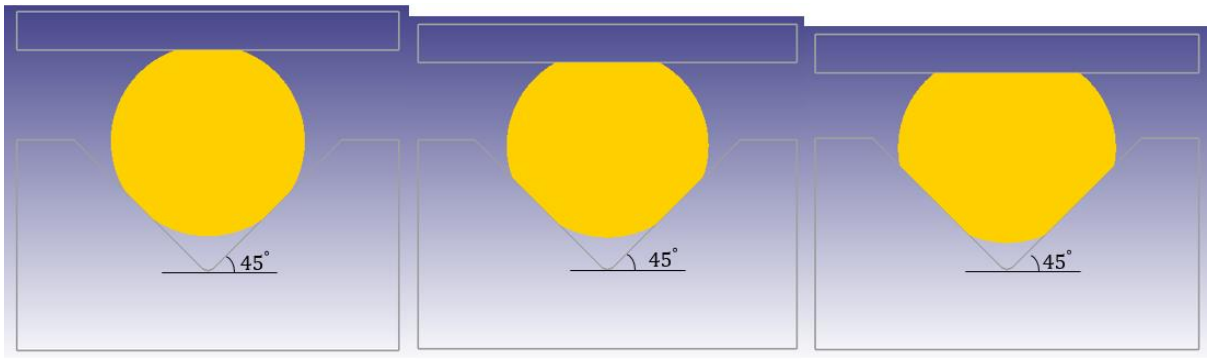

Fig.4
Schematic illustration of the FE mesh model after upsetting a billet, using bottom die angle 45° for $\delta = 1, 2, 3$ *mm*.

Variation of the predicted upper die half contact length and the arc radius values, *b* and *R*, based on the slab method of analysis and those of FE data, versus die stroke is shown in Fig. 5 for $R_0 = 10$ *mm*, $v_0 = 1$ *mm/s*, $m = 0.1$ and $\theta = 45^{\circ}$. As shown in this figure as the process proceeds, the contact length between the top die and the billet and the arc radius are increased and the values of theoretical predictions are in very good agreement with the results of FE data.

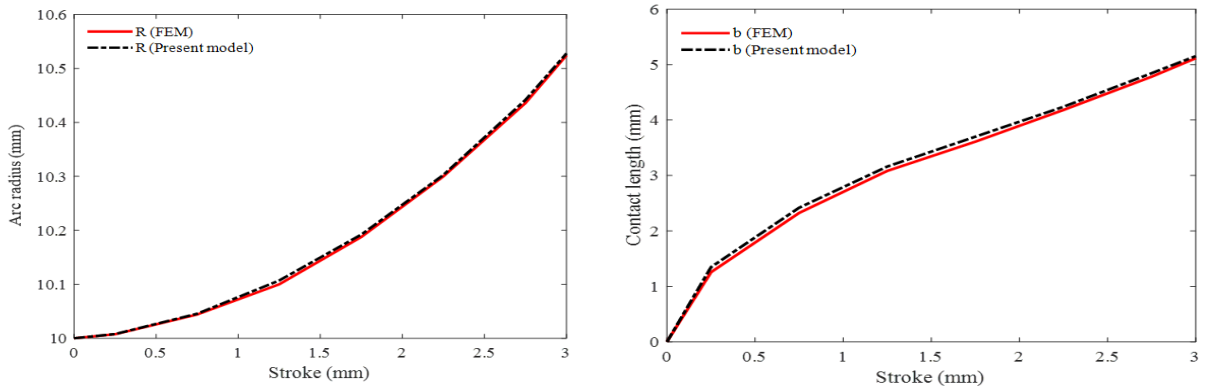

(a) Variation of the arc radius *R* versus upper die stroke (b) Variation of half contact length *b* versus upper die stroke

Fig.5
Variation of contact length *b* and the arc radius *R* versus upper die stroke, comparison of analytical results and FE data for $R_0 = 10$ *mm*, $v_0 = 1$ *mm/s*, $m = 0.1$ and $\theta = 45^{\circ}$.

In Fig. 6, the forming load variation during the process obtained from the slab method solution is compared with the FE data for $R_0 = 10$ *mm*, $v_0 = 1$ *mm/s*, $m = 0.1$ for two bottom die angles $\theta = 45^{\circ}$ and $\theta = 60^{\circ}$. As shown in this figure, the upsetting load increases as the process proceeds. It is observed that, the theoretically predicted load is

lower than the FE results, which is due to the nature of the slab method. From this figure, it is observed that the by increasing the stroke, the discrepancy between the results of the analytical solution and FEM increases. This is due to for small press stokes, contact surfaces between the material and the dies are small and the effects of the friction on the internal distortions is low but by increasing the stroke, the internal distortions increase and the discrepancy between the results of the analytical solution and FEM increases.

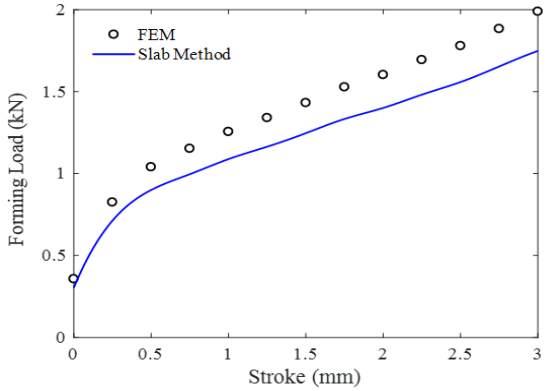

(a) Bottom die angle $\theta = 45^{\circ}$

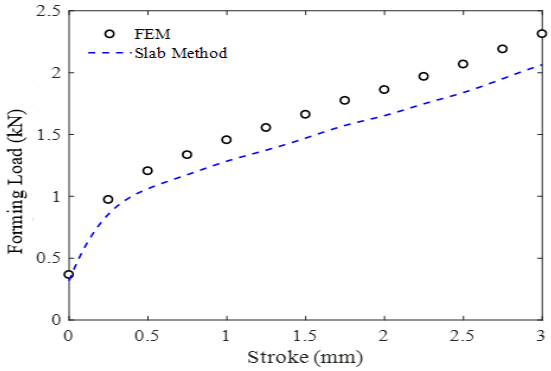

(b) Bottom die angle $\theta = 60^{\circ}$

Fig.6
Comparison of analytical and FE upsetting load-displacement curves for $R_0 = 10\ \ mm$, $v_0 = 1\ \ mm/s$, $m = 0.1$ and bottom die angles of $\theta = 45^{\circ}, 60^{\circ}$.

Variation of the forming load versus die stroke for three different die angles is plotted in Fig. 7. From this figure, it can be seen that by increasing of the bottom die angle θ, the forming load decreases.

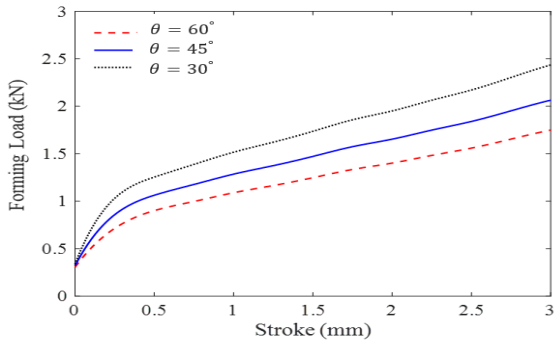

Fig.7
Comparison of analytical forming load-displacement curves for bottom die angles of $\theta = 30^{\circ}, 45^{\circ}, 60^{\circ}$.

The effect of the friction factor between the billet material and the dies on the forming load is also examined and it is shown in Fig. 8. It is clear that the load increases with the increasing of friction factor value but the effect of friction factor upon the forming load is not significant.

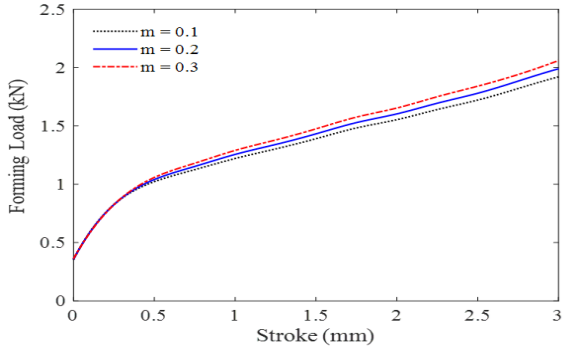

Fig.8
The effect of the friction factor on the forming load as a function of die stroke for $R_0 = 10\ mm$, $v_0 = 1\ mm/s$ and $\theta = 45^{\circ}$.

5 CONCLUSIONS

Based on the research work presented in the previous sections, the conclusions are as follows:

1. The developed analytical model is useful in the determination of the forming load.
2. The predicted deformation of the billet and the press loads are in good agreement with the FE simulation data.
3. In spite of the simplicity of the proposed solution, the relative difference between this solution and the solutions based on the FEM was comparatively small. This is a great advantage for engineering applications.
4. The use of the developed slab method code is very beneficial for determining the capacity of the required upsetting machine.

REFERENCES

[1] Oleg E.M., Alexander V.P., Marina A.M., Vitalii N.Z., 2015, Development of a new process for forging plates using intensive plastic deformation, *International Journal of Advanced Manufacturing Technology* **83**: 2159-2174.

[2] Nasmyth J., 1950, Improvements in forging iron, *Journal of the Franklin Institute* **50**: 404-408.

[3] Johnson W., 1958, Indentation and forging and action of Nasmyth's Anvil, *Engineer* **205**: 348-350.

[4] Keife H., Stahlberg U., 1980, Influence of pressure on the closure of voids during plastic deformation, *Journal of Mechanical Working Technology* **4**: 133-143.

[5] Stahlberg U., Keife H., Lundberg M., Melander A., 1980, A study of void closure during plastic deformation, *Journal of Mechanical Working Technology* **4**: 51-63.

[6] Vilotic D., Shabaik A.H., 1985, Analysis of upsetting with profiles dies, *Transactions of ASME Journal of Engineering Materials Technology* **107**: 261-264.

[7] Dudra S.P., Im Y.T., 1990, Analysis of void closure in open-die forging, *International journal of Machine Tools and Manufacture* **30**: 65-75.

[8] Dudra S.P., Im Y.T., 1990, Investigation of metal flow in open-die forging with different die and billet geometries, *Journal of Materials Processing Technology* **21**: 143-154.

[9] Lin S.Y., 2002, Stress analysis of upsetting with concave curve dies, *Journal of Materials Processing Technology* **123**: 36-44.

[10] Choi S.K., Chun M.S., Van Tyne C.J., Moon Y.H., 2006, Optimization of open die forging of round shapes using FEM analysis, *Journal of Materials Processing Technology* **172**: 88-95.

[11] Alexandrov S., Yusof M., 2009, An analysis of continued plane strain compression by the upper bound method, *ICCES* **10**: 11-23.

[12] Christiansen P., Hattel J.H., Kotas P., Laszlo V. , 2012, Modelling the void deformation and closure by hot forging of ingot castings, *International Conference on Ingot Casting, Rolling and Forging Technology*, Aachen, Germany.

[13] Banaszek G., Bajor T., Kawałek A., Garstka T., 2020, Analysis of the open die forging process of the AZ91 Magnesium alloy, *Materials* **13**: 3873.